

01 Apr 2022

## Analyzing the Influence of Imbalanced Two- or Three-Wire VHF LISN on Radiated Emissions from AC Cables

Hossein Rezaei

Morten Sorensen

Wei Huang

Daryl G. Beetner

*Missouri University of Science and Technology*, daryl@mst.edu

*et. al.* For a complete list of authors, see [https://scholarsmine.mst.edu/ele\\_comeng\\_facwork/4652](https://scholarsmine.mst.edu/ele_comeng_facwork/4652)

Follow this and additional works at: [https://scholarsmine.mst.edu/ele\\_comeng\\_facwork](https://scholarsmine.mst.edu/ele_comeng_facwork)

 Part of the [Electrical and Computer Engineering Commons](#)

---

### Recommended Citation

H. Rezaei et al., "Analyzing the Influence of Imbalanced Two- or Three-Wire VHF LISN on Radiated Emissions from AC Cables," *IEEE Transactions on Electromagnetic Compatibility*, vol. 64, no. 2, pp. 327 - 337, Institute of Electrical and Electronics Engineers, Apr 2022.

The definitive version is available at <https://doi.org/10.1109/TEMPC.2021.3111136>

This Article - Journal is brought to you for free and open access by Scholars' Mine. It has been accepted for inclusion in Electrical and Computer Engineering Faculty Research & Creative Works by an authorized administrator of Scholars' Mine. This work is protected by U. S. Copyright Law. Unauthorized use including reproduction for redistribution requires the permission of the copyright holder. For more information, please contact [scholarsmine@mst.edu](mailto:scholarsmine@mst.edu).

# Analyzing the Influence of Imbalanced Two- or Three-Wire VHF LISN on Radiated Emissions from AC Cables

Hossein Rezaei <sup>1</sup>, Member, IEEE, Morten Sørensen <sup>2</sup>, Senior Member, IEEE, Wei Huang, Member, IEEE, Daryl G. Beetner <sup>3</sup>, Senior Member, IEEE, and David Pommerenke <sup>4</sup>, Fellow, IEEE

**Abstract**—This article investigates using imbalanced two- and three-wire terminations for ac main cables, as suggested by the standard group. These terminations provide the basis for a new line impedance stabilization network (LISN) whose objective is to improve test repeatability between labs while also providing better estimation of real-world emissions. Standard balanced LISNs do not reproduce the imbalanced terminations seen in practice. An imbalanced two- or three-wire very high-frequency LISN was built, which can handle up to 15 A on each line. The LISN operates from 30 to 200 MHz and provides greater than 50-dB isolation between the input and output. The imbalanced termination allows the device to create a specified degree of conversion from differential-mode to common-mode current, which can increase radiated emissions. This conversion was evaluated to be as high as 12 dB in measurements of a power line communication device. 3-D full-wave simulations of two- and three-wire applications demonstrate that the radiated emissions from the prototype LISN and the ideal imbalanced termination are nearly equal. The new LISN was further evaluated to show promise for improving measurement reproducibility, reducing the standard compliance uncertainty by 6 dB in this study, from 15.5 dB in CISPR 16-4-1 to 9.5 dB with the LISN.

**Index Terms**—Common-mode impedance, radiated emissions, termination device, very high-frequency line impedance stabilization network (VHF LISN).

## I. INTRODUCTION

COMMON mode conducted emissions are typically measured using a line impedance stabilization network (LISN) [1]–[9]. An LISN is a filtering device providing a) isolation of

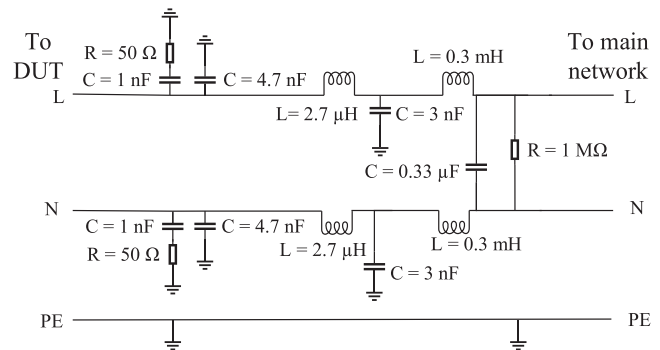


Fig. 1. Circuit diagram of a typical balanced VHF LISN [4], [7], [8].

the device under test (DUT) from ac power lines and related radio frequency (RF) disturbances, b) a well-defined reference impedance at the LISN DUT port; and c) the necessary power to the DUT. Standard LISNs use a balanced termination structure [3]–[9]. Round-robin testing for radiated emissions show that the average emissions differ by 4 dB when using a traditional balanced LISN (see Fig. 1) [3], [4], but those deviations in measurements were as large as +18/–10 dB when the DUT was plugged directly into the building mains [3], [4]. Although a goal of the balanced very high-frequency (VHF) LISN is to reduce variations among tests [1]–[9], a balanced termination is rarely available in practice, so real-world emissions may be higher than seen in many standardized measurements.

The LISN forms an impedance between the wires of the power cable and the chamber ground and, thus, can be used as a common-mode absorption device above 30 MHz. If the common-mode impedance of the LISN is between 50 and 300 Ω, most of the common-mode resonances of the power cable will be suppressed. Suppressing these resonances reduces the dependence of the emissions on the power cable routing, the specific impedance of the chamber's power connection, and the length of the power cord. While reducing this dependence is attractive for minimizing chamber to chamber variations, it also hides an important effect that causes radiation. In real installations, the differential-mode noise current is often larger than the common-mode noise current in a power cable, and real installations will have asymmetric common-mode impedances [10]–[12]. This

Manuscript received February 26, 2021; revised June 24, 2021 and August 12, 2021; accepted September 4, 2021. Date of publication October 4, 2021; date of current version April 14, 2022. This work was supported by the National Science Foundation under Grant IIP-1916535. (Corresponding author: Hossein Rezaei.)

Hossein Rezaei and Daryl G. Beetner are with the EMC Laboratory, Missouri University of Science and Technology, Rolla, MO 65409 USA (e-mail: hrr7d@mst.edu; daryl@mst.edu).

Morten Sørensen is with the Center for Industrial Electronics, Department of Mechanical and Electrical Engineering, University of Southern Denmark, 6400 Sønderborg, Denmark (e-mail: soerensen@sdu.dk).

Wei Huang is with the ESEMC Technology LLC, Rolla, MO 65401 USA (e-mail: info@esdemc.com).

David Pommerenke is with the Graz University of Technology, 8010 Graz, Austria, and also with Silicon Austria Lab's Graz EMC Lab, 8010 Graz, Austria (e-mail: david.pommerenke@tugraz.at).

Color versions of one or more figures in this article are available at <https://doi.org/10.1109/TEM.2021.3111136>.

Digital Object Identifier 10.1109/TEM.2021.3111136

asymmetry will convert differential-mode current into common-mode current, which can radiate. To mimic this effect, a defined asymmetry can be introduced into the VHF LISN.

Using an imbalanced termination will increase the common-mode emissions by about 10 to 15 dB up to 200 MHz (depending on the DUT) compared to using a balanced termination [11]. About 10-dB higher emissions were also reported for an imbalanced two-wire LISN compare to a balanced LISN over 0.5 to 30 MHz in [11]. To address the differential- to common-mode current conversion in a VHF LISN (30 to 200 MHz), the termination impedance should have a controlled imbalance to provide a defined degree of conversion from differential- to common-mode current. The standard group introduced an imbalanced termination for this purpose and suggested that an LISN with similar performance should be created for the 30- to 200-MHz frequency range [10].

In this article, an imbalanced LISN with the characteristics suggested by the works in [10]–[12] was designed, built, and analyzed to serve as the termination of the mains power during radiated EMI CISPR16/CISPR 35 testing [1]. This LISN was designed in Section II to supply power for imbalanced two- or three-wire measurements up to 15 A over a frequency range from 30 to 200 MHz. In Section III, a 3-D full-wave simulation with both differential- and common-mode excitations representing the DUT was used to illustrate the effect of the VHF LISN on radiated emissions on a typical test setup for two- or three-wire application. A study of differential- to common-mode current conversion was performed to verify the conversion ratio for an ideal imbalanced termination. In a real test setup, the differential- to common-mode current conversion is geometry dependent but not a fixed number. Measurements of a pair of power line communication devices were performed in Section IV to validate the performance of the LISN in a typical test setup and to demonstrate the level of differential- to common-mode current conversion for a real-word application. Discussions are presented in Section V. Finally, Section VI concludes this article.

## II. DESIGN OF AN IMBALANCED TWO- OR THREE-WIRE LISN

The following section will introduce the imbalanced two-wire and three-wire terminations suggested by the working group and the literature [10]–[12], provide evidence of the suitability of the proposed impedances, show the characteristics of the actual LISN that was built to use these terminations, and give the value of differential- to common-mode conversion for a practical test setup connected to the imbalanced two wire termination.

### A. Imbalanced Two- or Three-Wire Termination

The imbalanced two- and three-wire terminations proposed by the works in [10]–[12] are shown in Fig. 2(a) and (b), respectively. The termination characteristics for two-wire applications were specified as follows.

- 1) Common-mode impedance  $Z_{CM}$  of  $150\ \Omega \pm 10\%$  from 30 to 200 MHz, which defines the impedance between the line (L) and neutral (N) wires and the ground-plane, when the line and neutral wires are shorted together.

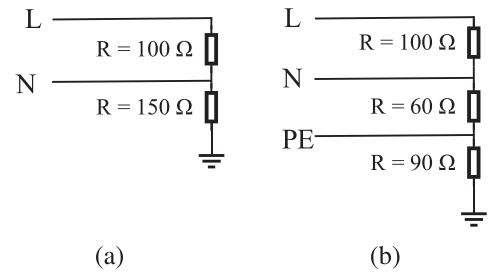


Fig. 2. Proposed imbalanced terminations. (a) Two-wire termination. (b) Three-wire termination.

- 2) Differential-mode impedance  $Z_{DM}$  of  $100\ \Omega \pm 10\%$  from 30 to 200 MHz, which defines the impedance between the line and neutral wires when the neutral wire is shorted to the ground plane.
- 3) Impedance between the line and ground plane of  $250\ \Omega \pm 20\%$  from 30 to 200 MHz.

The termination characteristics for three-wire applications were specified as follows.

- 1) Common-mode impedance  $Z_{CM}$  of  $90\ \Omega \pm 10\%$  from 30 to 200 MHz, which defines the impedance between the line, neutral, and protective earth (PE) wires (shorted together) and the ground plane.
- 2) Differential-mode impedance  $Z_{DM}$  of  $100\ \Omega \pm 10\%$  from 30 to 200 MHz, which defines the impedance between the line wire and the neutral and PE wires, when the neutral and PE are shorted to the ground plane.
- 3) Tertiary-mode impedance  $Z_{TM}$  of  $60\ \Omega \pm 10\%$  from 30 to 200 MHz, which defines the impedance between the line and neutral wires shorted together, and the PE wire and ground plane shorted together.

The working group [10]–[12] chose a 150- $\Omega$  two-wire common-mode impedance to suppress standing waves in the DUT power. The geometry of a power cable does not allow for easily assigning a common-mode impedance, as the wave structure deviates strongly from a TEM mode wave, but it has been shown that termination impedances in the range of 50 to 200  $\Omega$  suppress standing waves well [13]. Although not exact, using a common-mode impedance of about 150  $\Omega$  [see Fig. 2(a)] will provide results similar to those observed in [13] and minimal common-mode resonances will occur [13]–[15].

A 90- $\Omega$  termination was selected for the slightly thicker three-wire cables [10]. The 100- $\Omega$  differential impedance was chosen to mimic the impedance of a typical transmission line (TL) formed by the line and neutral wires [10]. To provide evidence for the validity of this selection, 48 different power cables were measured using a time-domain reflectometer (TDR) (see Fig. 3). Eleven were two wire cables, and 37 were three wire cables.

The impedance value was recorded between the short discontinuity at the beginning of the coax to cable transition and the end of the cable, which was left open. As shown in Fig. 3, a small adapter was made to connect the coax cable to the power cord, which causes a short discontinuity but does not affect the TDR measurement, as we record the differential impedance between

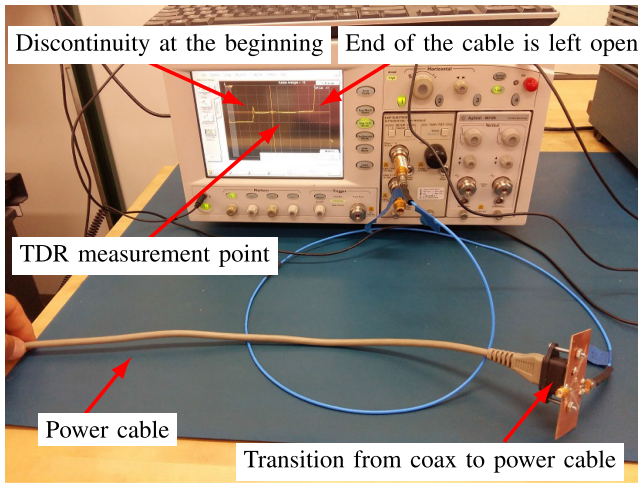


Fig. 3. Measurement setup for power cord cable differential-mode impedance using TDR.

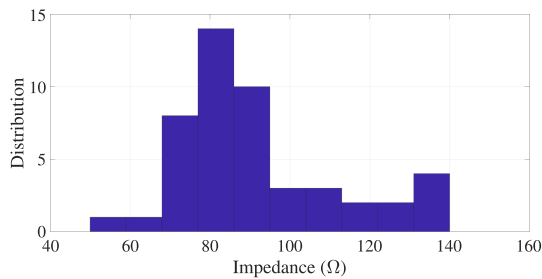


Fig. 4. Distribution of differential-mode impedances for a set of power cables.

the two lines after that discontinuity. The length of the cables is not important as we look at the differential-mode impedance provided by two wires ( $L$  and  $N$ ).

The distribution of the characteristic impedances is shown in Fig. 4. The distribution shows the typical value of the differential impedance is close to 100  $\Omega$ , as suggested by the working group [10]–[12]. In the tertiary mode, the line and neutral wires are shorted and driven against the PE and ground (shorted). The line and neutral wires together as a larger “signal” conductor compared to the differential mode case, so the TL impedance is expected to be smaller. A value of  $Z_{TM} = 60 \Omega$  was chosen for this reason [10].

### B. Prototype Imbalanced Two- or Three-Wire LISN

An imbalanced LISN was designed to meet the specifications of the working group. Additional requirements for the designed LISN are listed in Table I. Fig. 5 shows the LISN’s circuit diagram. The capacitor inductor networks in Fig. 5 ( $L_1$ ,  $C_3$ ,  $L_4$ , and  $L_2$ ,  $C_4$ ,  $L_5$ ) were built to provide the required 50 dB of isolation of the DUT from the mains network at higher frequencies and provide a good connection to the building mains at 50 to 60 Hz. The capacitors  $C_1$  and  $C_2$  were made sufficiently small to isolate the line and neutral wires from each other and the PE at 50 to 60 Hz, but to allow resistors ( $R_1$ ,  $R_2$ , and  $R_3$ ) to define the termination from 30 to 200 MHz. While the schematic in Fig. 5 should meet the specifications of the working group, validation

TABLE I  
CHARACTERISTICS OF PROPOSED IMBALANCED TWO- OR THREE-WIRE VHF LISN

Parameter	Characteristic
Frequency	30 MHz to 200 MHz
Network impedance	Two wire: $Z_{DM} = 100 \Omega$ , $Z_{CM} = 150 \Omega$ Three-wire: $Z_{DM} = 100 \Omega$ , $Z_{CM} = 90 \Omega$ , $Z_{TM} = 60 \Omega$ . ( $\pm 10\%$ on magnitude and $\pm 30^\circ$ on phase)
Maximum current	15 A RMS
Maximum AC voltage	250 V, 50 Hz to 60 Hz
Isolation on each line	Better than 50 dB

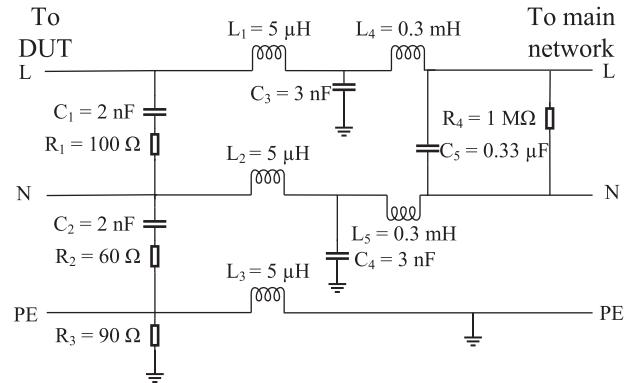


Fig. 5. Circuit diagram of the proposed two- or three-wire imbalanced LISN.

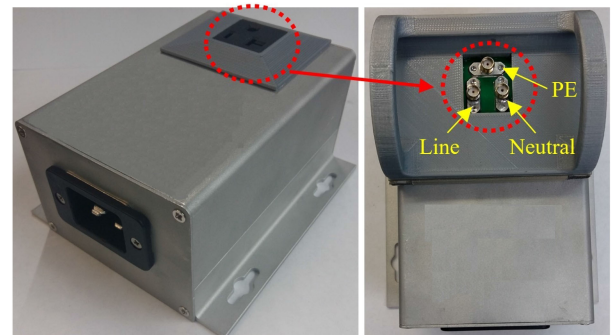


Fig. 6. Prototype of imbalanced two- or three-wire VHF LISN.

is required since parasitics could alter the actual impedances looking into the LISN.

The six impedances specified by the working group could not be measured directly, since they require a floating measurement and different parasitics will be involved in each measurement. To determine the impedances, a combination of measurement and postsimulation was used. Three-port  $S$ -parameter measurements were made looking into each terminal of the LISN. A test fixture (see Fig. 6) was built to connect the LISN to the vector network analyzer for the three port  $S$ -parameter measurement. The measured  $S$ -parameter matrix was imported into advance design system (ADS) [16] to calculate the six specified impedances. The measured impedances and those suggested by the working group are shown in Figs. 7, 8, 9, and 10. The magnitudes of the measured impedances are all within the ranges proposed by the working group [10]–[12]. While the working group does



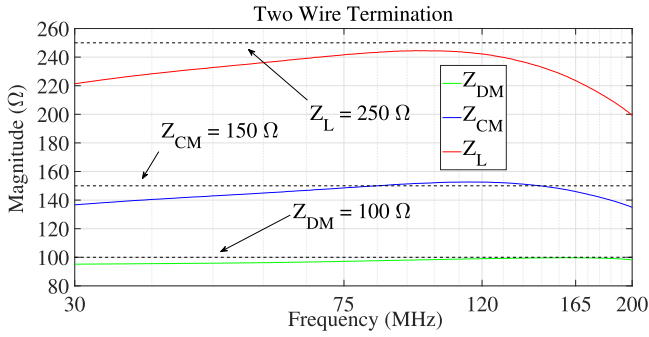


Fig. 7. Magnitude of the impedance of the prototype LISN for a two-wire application. The deviation from the suggested value is within 10% for  $Z_{CM}$  and  $Z_{DM}$  and 20% for  $Z_L$  from 30 to 200 MHz.

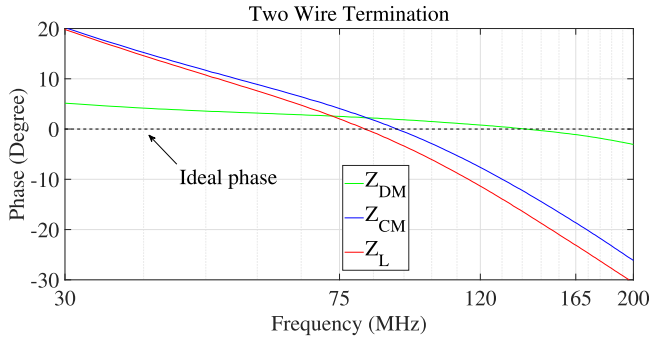


Fig. 8. Phase of the impedance of the prototype LISN for a two-wire application. The phase deviates from the phase of an ideal resistor by less than  $30^\circ$  from 30 to 200 MHz.

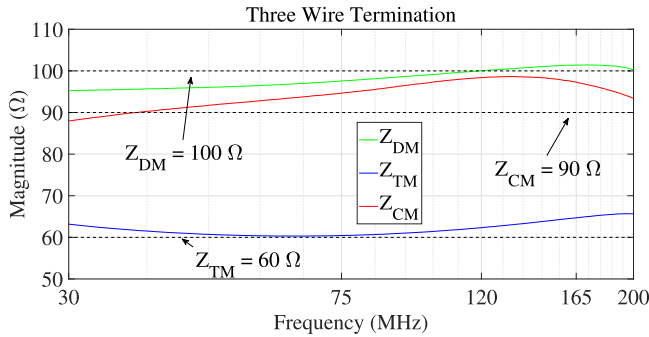


Fig. 9. Magnitude of the impedance of the prototype LISN for a three-wire application. The deviation from the suggested value is within 10% from 30 to 200 MHz.

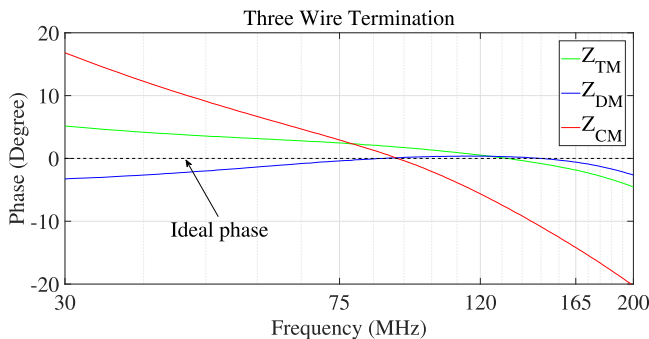


Fig. 10. Phase of the impedance of the prototype LISN in a three-wire application. The phase deviates from the phase of an ideal resistor by less than  $30^\circ$  over 30 to 200 MHz.

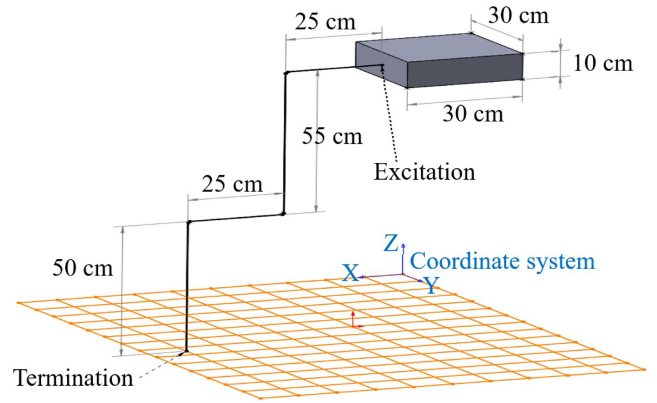


Fig. 11. 3-D full-wave simulation setup for two wires.

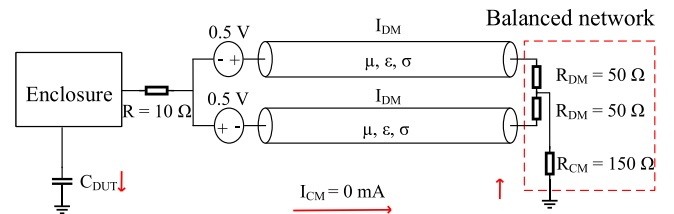


Fig. 12. Balanced impedance to ground for a two-wire setup.

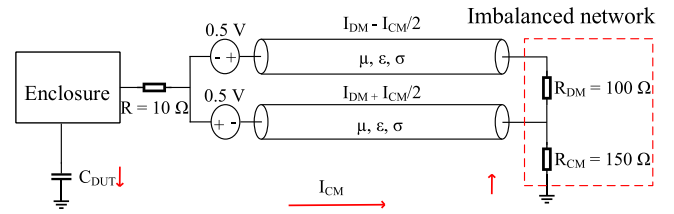


Fig. 13. Imbalanced impedance to ground for a two-wire setup.

not explicitly specify the phase, the measured phase is within about  $30^\circ$  of the ideal  $0^\circ$  phase for a resistive termination. More important than the variations in the actual impedance is its impact on the radiated fields. It will be shown in Section III that up to  $30^\circ$  variation in phase plus 10% variation in the magnitude of the LISN impedance will cause less than  $\pm 3$  dB variation in the radiated emissions, which is acceptable in EMC applications. These results suggest a  $\pm 10\%$  change in magnitude and  $\pm 30^\circ$  in phase is an appropriate limit for defining the impedance of an imbalanced VHF LISN.

### C. Impact of Imbalance on Differential- to Common-Mode Conversion

An LISN is a filtering device providing the following:

- 1) isolation of the DUT from ac power lines and related RF disturbances;
- 2) a well-defined reference impedance at the LISN DUT port, which is isolated from the main network;
- 3) the necessary power supply to the DUT.

Looking from the DUT side, the common-mode impedance in the two-wire imbalanced LISN investigated is  $150 \Omega$  [see Fig. 2(a) and 13]. However, the common-mode impedance of

a balanced LISN is about  $50\ \Omega$  as seen from the DUT side. For both LISNs, the differential-mode impedance in the two-wire setup is  $100\ \Omega$  [11], [12].

Testing without an imbalanced termination misses the important differential- to common-mode current conversion that may occur when the product is connected to a real ac mains network. The impact of the imbalanced LISN on differential- to common-mode conversion was demonstrated using a 3-D full-wave model of a typical test setup. The model shown in Fig. 11 illustrates a typical radiation test setup [1]. The DUT is represented with a solid metal box ( $30\text{ cm} \times 10\text{ cm} \times 30\text{ cm}$ ) located 1 m above an infinite ground plane. The box is connected to a 1.5-m power cable. The wires in the cable were driven with a 1-V differential source with zero-output impedance, as shown in Figs. 12 and 13. The sources were connected to the DUT chassis with a low impedance ( $10\ \Omega$ ). This impedance is intended to represent a poor connection of a shield to the chassis. This connection was compared to a  $1\text{-}\Omega$  connection, which showed that this selection of the connection impedance does not significantly influence the conclusions drawn from the simulation.

A typical power cord geometry was used having a 1.62-mm wire diameter, a 0.89-mm-thick PVC insulation, and a PVC jacket with a diameter of 9.5 mm. The metal to metal distance between the wires was 2.35 mm. This distance forms a TL of about  $80\ \Omega$  between the line (L) and neutral (N).

Circuit schematics of the full-wave structure with balanced and imbalanced terminations are shown in Figs. 12 and 13, respectively. The balanced or imbalanced terminations were chosen similar to those recommended for the LISN (see Fig. 2). The capacitance between the DUT enclosure and ground is about  $C \approx 50\text{ pF}$ , depending on the size of the DUT. This capacitance creates an impedance of about 15 to  $100\ \Omega$  from 30 to 200 MHz, which is on the order of the  $150\text{-}\Omega$  common-mode termination  $R_{CM}$ , so that nonnegligible common-mode current could flow. Simple models without TLs and an estimated value of the coupling capacitance between the DUT and ground can be evaluated in [11]. Each wire is driven with an identical 0.5-V voltage source if opposite sign is creating a 1-V differential-mode source, which drives differential-mode current. As indicated in Fig. 12, there is no common-mode current when using a balanced termination, whereas the imbalanced termination will cause differential- to common-mode conversion of current (see Fig. 13), which will increase radiated emission. According to the works in [10]–[12], real installations have imbalances, which should be reproduced by the EMC test setup.

To calculate the amount of differential- to common-mode conversion, the full-wave model in Fig. 11 was simulated with an imbalanced two-wire termination (see Fig. 13) over a frequency range from 30 to 200 MHz, as shown in Fig. 14. The differential-mode current reduces with frequency since the  $80\text{-}\Omega$  TL is terminated into  $100\ \Omega$ . Of course, for a different cable geometry, the differential-current (blue curve in Fig. 14) might be slightly different but that should not affect the current ( $< 10\%$  variation) as long as the differential-mode impedance is between 80 to  $100\ \Omega$ .

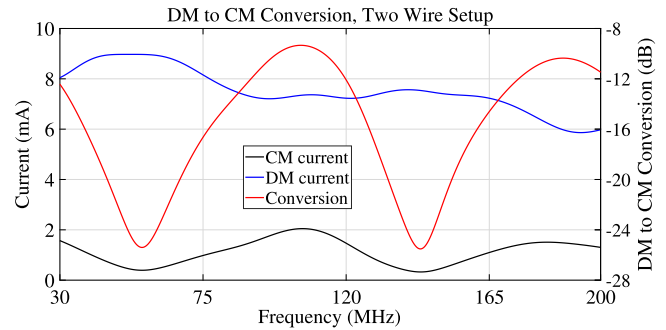


Fig. 14. Current flowing in an imbalanced two-wire termination. Plots in blue and black show the current in the individual wires. The plot in red shows the differential- to common-mode conversion ratio.

TABLE II  
CST SETTINGS FOR FULL-WAVE SIMULATION

Description	Setting
Frequency	30 MHz to 200 MHz
Background	Vacuum
Boundaries	Open (add space) in all directions except at Ymin which is electric ( $E_t = 0$ )
Field Monitor	Farfield / RCS, Transient Broadband
Setup Solver	Time Domain Solver
Post Processing	E-field, 3D, Max at 10 m distance

The common-mode current is affected by the structural length and fluctuates around 1 mA. The differential- to common-mode conversion can be measured by the ratio of the incident differential-mode power to the resulting power in the common mode as

$$C_{DM\text{ to }CM} = \frac{R_{CM} \cdot I_{CM}^2}{R_{DM} \cdot I_{DM}^2}. \quad (1)$$

The differential- to common-mode conversion ratio has been reported to be about  $-10$  to  $-15\text{ dB}$  for an imbalanced CDNE-M [11]. The actual conversion ratio obtained through full-wave simulation, however, is somewhat geometry dependent and varies from  $-9$  to  $-25\text{ dB}$ , as shown in Fig. 14. For a three-wire application [see Fig. 2(b)], the maximum differential- to common-mode conversion was similarly evaluated to be about  $-19\text{ dB}$ . The conversion is smaller for three wires than two, because current will return not only via the ground plane, but also in the PE wire. The portion that returns in the PE wire does not contribute to the common-mode current.

### III. RADIATED EMISSION USING THE IMBALANCED TWO- OR THREE-WIRE VHF LISN

To demonstrate the impact of the imbalanced LISN on radiated emissions, emissions were simulated using the full-wave model shown in Fig. 11. As shown in Section II-B, the impedances of the actual LISN vary about the ideal values due to unintended parasitics. Simulations were performed using the ideal LISN termination impedances and the realized values, as well as short and open terminations to show performance at the extremes. Table II summarizes all the settings used in the computer simulation technology (CST) Studio Suite. Simulation

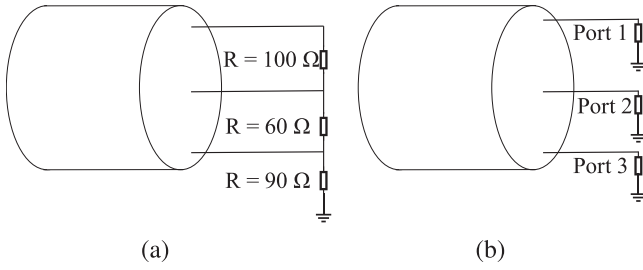


Fig. 15. Three-wire terminations used in full-wave simulation. (a) Three-wire imbalanced termination with lumped elements. (b) Termination with three  $S$ -parameter ports.

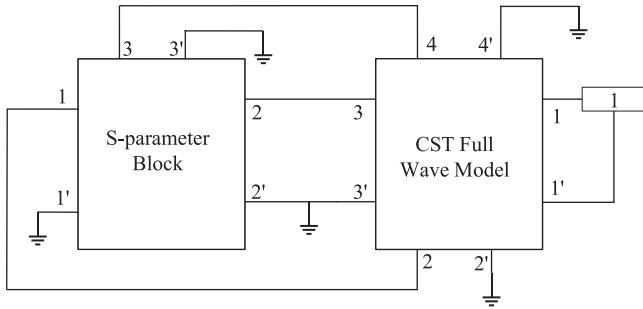


Fig. 16. CST true transient EM or circuit cosimulation with  $S$ -parameter block.

with the realized termination impedances was accomplished using the cosimulation feature of CST with the measured  $S$ -parameters. This feature combines the 3-D full-wave simulation with a circuit simulation or measurement [18] to simultaneously solve for the EM fields and the circuit characteristics. To ensure correct cosimulation, the following simulation procedure was used.

- 1) The setup shown in Fig. 11 was simulated with the ideal termination impedances represented as lumped elements [see Fig. 15(a)]. This simulation demonstrates the ideal performance of the imbalanced LISN and provides a reference for validation of the cosimulation approach.
- 2) A second simulation was performed using the ideal terminations with cosimulation [see Fig. 15(b)], where the excitation and the loads were replaced with  $S$ -parameter ports. Using the CST design studio cosimulation feature shown in Fig. 16, the excitation was connected to the source port and an  $S$ -parameter block representing the loads was connected to the load ports. An  $S$ -parameter block evaluated for ideal terminations [see Fig. 17(a)] was used to verify the procedure against the reference result from step 1.
- 3) After successful validation, the  $S$ -parameter matrix measured on the prototype was used to calculate the radiated emissions.

Radiated emissions were also evaluated for short and open terminations, when all the impedances on the termination side were replaced with open or short. The radiated emission was evaluated for all cases at a distance of 10 m. Results were evaluated for both common- and differential-mode excitations.

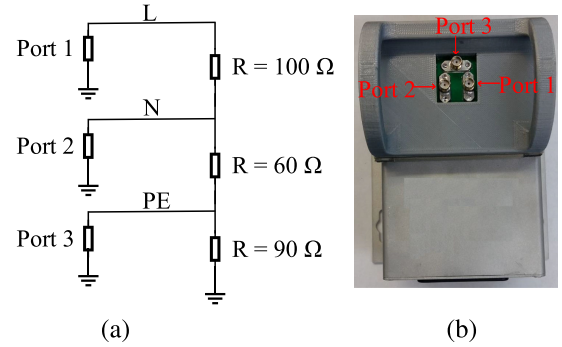


Fig. 17. (a) Port definition for ADS simulation of an ideal three-wire imbalanced termination. (b) Port definition for full  $S$ -parameter measurement of the prototype imbalanced two- or three-wire VHF LISN.

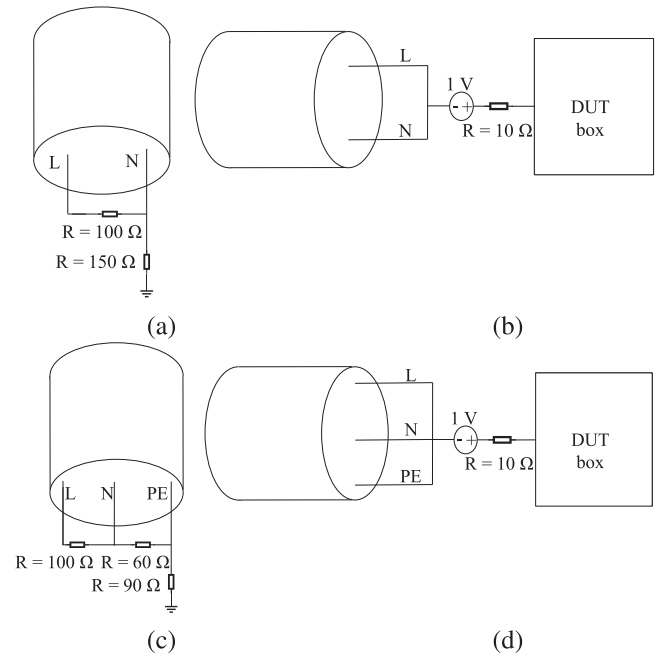


Fig. 18. Terminations used for common-mode simulations. (a) Two-wire imbalanced termination. (b) Common-mode excitation. (c) Three-wire imbalanced termination. (d) Common-mode excitation.

#### A. Common-Mode Excitation With Imbalanced VHF LISN

The schematic for the simulation setups with a common-mode excitation and ideal imbalanced two- and three-wire terminations are shown in Fig. 18. The maximum simulated far-field radiation for the three-wire setup with the studied terminations is shown in Fig. 19.

Strong resonances were observed for open and short terminations. The first peak is around 50 MHz, which is below the quarter wavelength frequency for a 1.5-m wire length, because the 50-pF capacitance between the DUT enclosure and the surroundings. At resonances, the radiation can exceed the radiation from the ideal termination by up to 15 dB. The 90- $\Omega$  common-mode termination impedance effectively damps resonances and in that regard seems reasonable with respect to repeatability. These results are in agreement with the previous study on the effect of common-mode impedance on radiation [2]. As shown

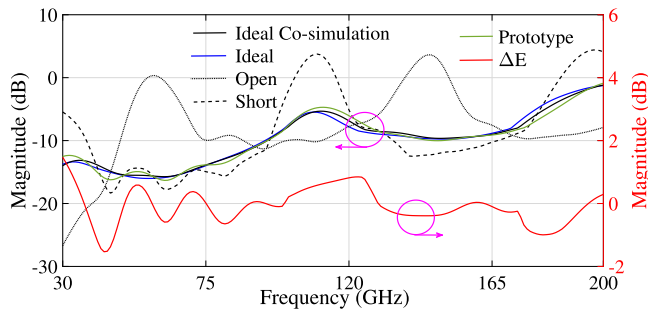


Fig. 19. Full-wave simulation result showing the radiated emissions from the three-wire setup with common-mode excitation. The difference between the radiation using the ideal and the real termination is  $\Delta E < 2$  dB up to 200 MHz.

in Fig. 19, the termination impedance is important at lower frequencies, but is not as significant at higher frequencies due to the increasing electrical length of the wire and the impact of damping due to radiation.

The black and blue curves in Fig. 19 show the results using the cosimulation technique and using standard simulations with ideal terminations. The two curves are nearly identical ( $< 1$  dB difference). The green curve shows the radiated emissions using the measured termination  $S$ -parameters from the prototype. Comparing the blue and green curves, the radiated emissions from the real LISN is nearly equal to the radiation seen for the ideal termination case. Similar results were seen for the two-wire common-mode case [e.g., using terminations as in Fig. 18(a) and (b)]. The radiated emissions from the prototype LISN are close to the emissions from an “ideal” imbalanced LISN with less than 2-dB error up to 200 MHz (red curve in Fig. 19).

### B. Differential-Mode Excitation With Imbalanced VHF LISN

Fig. 20 shows the differential-mode source excitation and the imbalanced termination in two- and three-wire setups. For both setups, the DM excitation was 1 V with  $0\text{-}\Omega$  output impedance. A low impedance ( $10\text{ }\Omega$ ) was selected to connect the wire to the DUT to represent a moderately poor connection to the enclosure. The radiated emissions from the two- and three-wire setups with differential-mode excitation are shown in Figs. 21 and 22, respectively.

When the ends of the wires on the termination side are open or shorted to the ground plane, the structures are symmetric. In this case, there is little common-mode current flowing in the circuit and very low radiation is observed. Large resonances are shown with open or short terminations because the source impedance is  $0\text{ }\Omega$  and there is little loss in the system. Resonances would be damped in this case with a larger source impedance. When using imbalanced terminations, there is noticeable differential to common-mode conversion for both the two- or three-wire case, which significantly increases the radiated emissions. As shown in Figs. 21 and 22, the results using cosimulation and using the standard EM simulation with ideal terminations are nearly identical. The difference between the radiation evaluated using the measured  $S$ -parameters from the prototype and using ideal terminations was less than a 3.2 dB up to 200 MHz (red curves in Figs. 21 and 22).

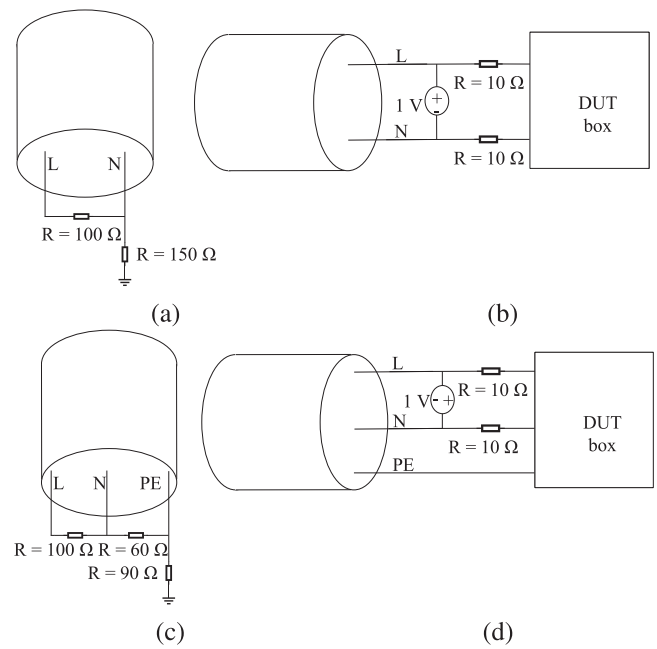


Fig. 20. Terminations used for differential-mode simulations. (a) Two-wire imbalanced termination. (b) Differential-mode excitation for two-wire setup. (c) Three-wire imbalanced termination. (d) Differential excitation for three-wire setup.

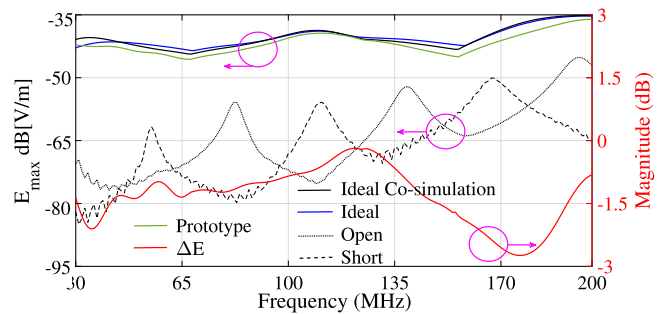


Fig. 21. Full-wave simulation result showing the radiated emission for the two-wire setup with differential-mode excitation. The difference between the radiation using the ideal and the real termination is  $\Delta E < 2.5$  dB up to 200 MHz.

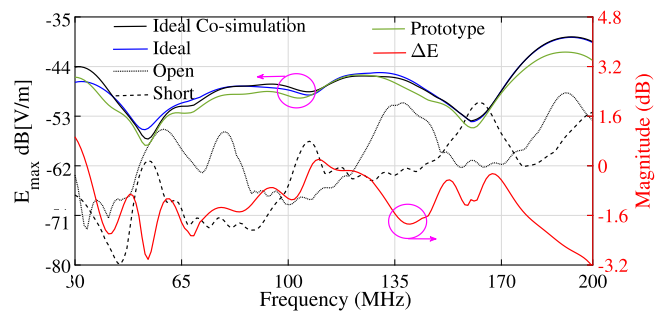


Fig. 22. Full-wave simulation result showing the radiated emission for the three-wire setup with differential excitation. The difference between the radiation using the ideal and the real termination is  $\Delta E < 3.2$  dB up to 200 MHz.



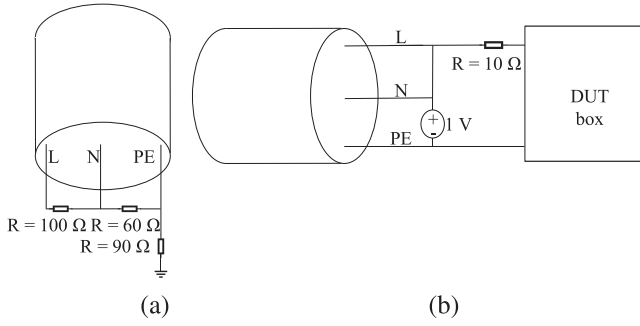


Fig. 23. Terminations used for tertiary-mode simulations. (a) Three-wire imbalanced termination. (b) TM excitation.

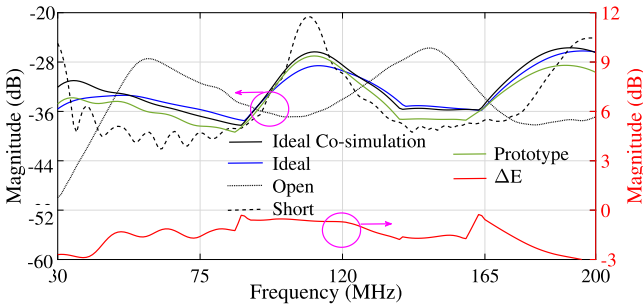


Fig. 24. Full-wave simulation results showing the radiated emissions for the three-wire setup with tertiary-mode excitation. The difference between the radiation using the ideal and the real termination is  $\Delta E < 3$  dB up to 200 MHz.

### C. Tertiary-Mode Excitation With Imbalanced VHF LISN

Fig. 23 shows the tertiary-mode source excitation and imbalanced terminations for the three-wire setup. The excitation is 1 V with zero output impedance. The radiated emissions with a tertiary-mode excitation are shown in Fig. 24. When the wires are open or short, the structure creates a highly resonant system. In the presence of terminations, these resonances will be dampened, regardless of their source. The radiation of the prototype is very close to the radiation with an ideal termination, with less than 3-dB error up to 200 MHz (red curve in Fig. 24).

### D. Impact of Termination Condition on Measurement Uncertainty of Imbalanced VHF LISN

The results of radiated emission measurements are affected by the uncertainties listed in [20] and [21]. This section investigates the impact and degree of influence of mains cable termination conditions on the standards compliance uncertainty (SCU) [20], [21]. The SCU is dependent on termination conditions over the frequency range where power cable radiation dominates [20]. Considering the tolerance of the termination impedance, the variation of the emission levels can be calculated, which also allows calculation of the measurement uncertainty influence [20].

The sensitivity of the radiation behavior of the LISN to deviations in the magnitude and phase of the terminating impedance from the ideal case should be analyzed to understand their impact on the SCU. Uncertainty is considered in the CISPR 16-4-1 standard [21]. Here, the average combined standard uncertainty

( $U_{c\text{-scu}}$ ), including the terminating condition of the main cable, is defined to be

$$U_{c\text{-scu}} = \sqrt{U_{c\text{-MIU}}^2 + U_a^2 + U_b^2 + U_c^2} \quad (2)$$

where CISPR/TR 16-4-1 specifies [19], [20] the following.

- 1)  $U_{c\text{-MIU}}$ , combined measurement instrumentation uncertainty, of 2.5 dB.
- 2)  $U_a$ , uncertainty from the main cable arrangement, of 3.5 dB. This value will depend on the termination conditions.
- 3)  $U_c$ , uncertainty in the operating condition of DUT, of 1.7 dB.
- 4)  $U_b$ , the uncertainty in termination conditions.

Assuming a rectangular probability distribution for the uncertainty of the cable terminating conditions, which is considered in CISPR 16-4-1 [21], the uncertainty in the terminating condition is given by [20]

$$U_b = \frac{E_{\max} - E_{\min}}{2 \cdot \sqrt{3}} = \frac{\Delta E}{2 \cdot \sqrt{3}} \quad (3)$$

where  $E_{\max}$  and  $E_{\min}$  are the maximum and minimum electric field strengths in dB  $\mu$  V/m, respectively. If we consider the maximum deviation due to the termination condition of the prototype up to 200 MHz to be 3.5 dB (see Fig. 22 for a three-wire termination with DM excitation), the uncertainty in the terminating condition  $U_b$  is only 1 dB. Using (2), the average combined standard uncertainty ( $U_{c\text{-scu}}$ ) is 4.7 dB. The expanded standard uncertainty  $U_{\text{scu, VHF-LISN}}$  is [20]

$$U_{\text{scu, VHF-LISN}} = 2 \cdot U_{c\text{-scu}} = 9.5 \text{ dB}. \quad (4)$$

Compared to the 50- $\Omega$  LISN in [20] with an expanded standard uncertainty  $U_{\text{scu, VHF-LISN}} = 12 \sim 13$  dB, the expanded standard uncertainty of the imbalanced two- or three-wire VHF LISN has been improved by about 2.5 dB. Compared to the 15.5-dB uncertainty defined in CISPR 16-4-1 [21], the SCU for the imbalanced two- or three-wire VHF LISN is improved by about 6 dB. It should be noted that only a single device was studied here, and results may change with other devices.

## IV. VALIDATION THROUGH MEASUREMENT

The effect of the differential- to common-mode conversion was investigated using a power line communication device. The goal was to investigate the impact of termination conditions on emissions with a DUT that uses a strong differential-mode signal to transmit data over power lines [11], [12]. The test used different termination conditions, a balanced LISN, an imbalanced LISN, and no LISN. A balanced LISN (see Fig. 1) was prototyped to compare with the imbalanced LISN. The balanced LISN had a 50- $\Omega$  impedance on each line with less than 1.5- $\Omega$  variations in magnitude and less than 5° variations in phase over the frequency range from 30 to 200 MHz.

A block diagram of the measurement setup inside the semi-anechoic chamber is shown in Fig. 25. The two DUTs are HD power line adaptors (PLA5456), which communicate with each other through power lines. The measurement setup is shown in Fig. 26. The DUTs and LISN are mounted on the floor

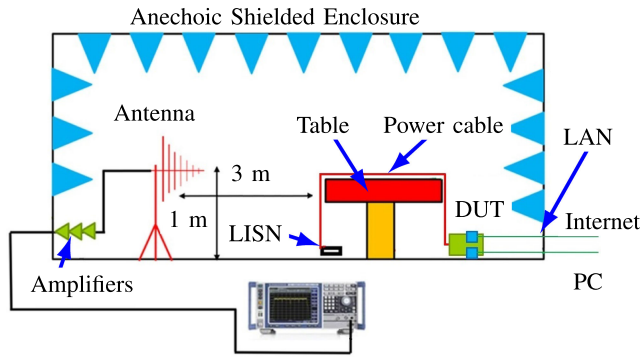


Fig. 25. Block diagram of measurement setup with a power line communication device inside a semianechoic chamber (SA setting: Frequency: 30 to 200 MHz, Trace: MaxHold, Detector: Positive Peak, RBW: 100 kHz).

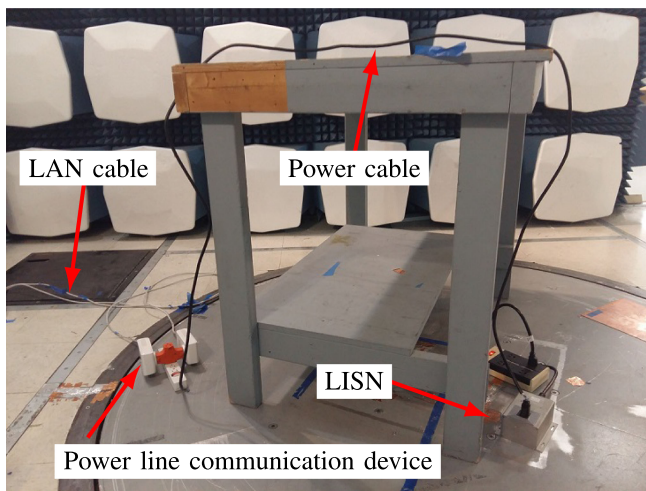


Fig. 26. Measurement setup with a power line communication device inside an anechoic chamber.

such that the power cable produces a loop with the maximum radiated emissions toward the antenna. A personal computer (PC) was needed to communicate with the DUT. To generate the highest differential-mode current, the DUT was operated under its maximum data rate. The measurement was performed for both horizontal and vertical polarizations and with 1- to 4-m scan heights of the antenna. The table was also partially rotated to capture the maximum radiation.

The goal was to show the differential- to common-mode conversion by using an imbalanced LISN, but also to show the impact of connecting the LISN to different power nets, as well as to show the impact of the power nets on emissions when no LISN was used. Connecting the LISN to different power nets helps to show if it has reproducibility issues. Different power networks were created by adding a soldering iron, a linear dc power supply, different wires with terminations, such as 2 nF, power cords, and strip lines, to the outlet inside the chamber.

Changing the power net before the LISN should have no effect, as the LISN isolates well. With different termination impedances, however, the radiation should change noticeably if no LISN is used. While different emissions are expected from a balanced or imbalanced LISN, both are expected to

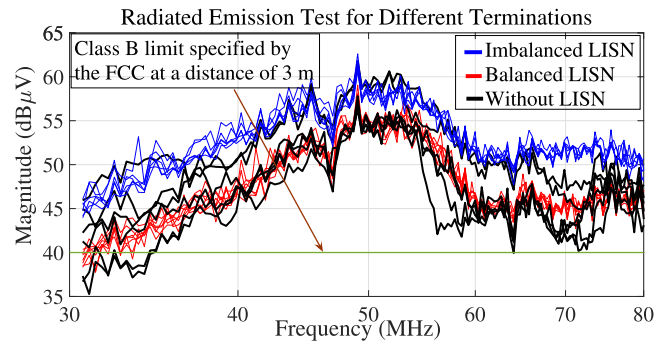


Fig. 27. Measured radiated emissions for power line communication devices using different terminations. The device has no differential-mode energy above 80 MHz.

generate somewhat stable curves because both LISNs isolate the DUT from the power net. Higher radiation is expected using an imbalanced LISN rather than by using a balanced LISN, since the imbalanced LISN converts differential-mode current into common-mode current. Radiation results for all power networks and using three different termination conditions (balanced LISN, imbalanced LISN, and no LISN) are shown in Fig. 27. When both power line communication devices are ON, the broadband signal below 80 MHz is representative of the data transfer from the DUT. The DUT has no differential-mode energy above 80 MHz. Some observations are (a) when not using an LISN, the radiated emissions vary by up to 12 dB, since the termination is not controlled. (b) with a balanced or an imbalanced LISN, radiation has less than 3-dB variation, because the LISNs isolate the network and provide a well-defined termination. (c) the conversion with the imbalanced LISN is as high as 12 dB. (d) the imbalanced LISN generates emissions that are close to the worst of the measured emissions when connecting directly to the power networks, and (e) both LISNs have no reproducibility issues.

Neither impedance, nor conversion, has been characterized for the chamber used for measurement. Therefore, the observed variation in radiated emission is expected to be large  $\Delta E > 10$  dB. However, both balanced and imbalanced LISNs have controlled terminations and will not cause reproducibility problems because the data have less than 3-dB variation for different power networks. In general, the data show that for a device that has a strong differential-mode current, the imbalanced LISN brings the emissions to a more realistic level. The result from the balanced LISN ignores the differential- to common-mode conversion and gives unrealistically lower emission.

The conversion of course should correlate to the currents on the wires. The common-mode and differential-mode currents have been measured with a F65 current clamp at a few points along the cables. The maximum current has been captured and the conversion was calculated as the difference between the maximum common-mode current when the cable was terminated with balanced and imbalanced LISNs.

Similarly, the radiated emission conversion was calculated as the difference between the maximum radiated emission when the cable was terminated with balanced and imbalanced LISNs.

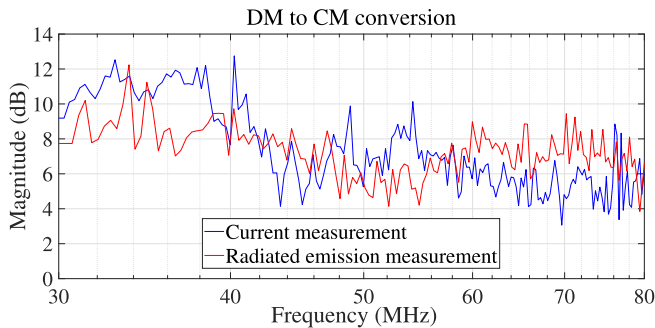


Fig. 28. Differential- to common-mode conversion from current and radiated measurements. The device does not use frequencies above 80 MHz.

Fig. 28 shows differential-mode to common-mode conversion, which is calculated from both current (blue curve) and radiated emission (red curve) measurement using balanced and imbalanced LISN. As shown in Fig. 28, the conversion calculated from radiated emission and the common-mode current are quite similar, i.e., this plot validates the conversion ratio with two different quantities, e.g., current, and radiated emissions. Above 80 MHz, the observed differences between the common-mode current for both balanced and imbalanced LISNs are almost zero because the DUT has no transmit energy. At the lower frequency band, the conversion is as high as 12 dB for both radiated emission and common-mode current.

## V. DISCUSSION

Imbalanced LISNs can be designed for different target impedances. The LISN analyzed in this article was designed for a 150- $\Omega$  common-mode impedance, as suggested in the literature [10]–[12]. This impedance can strongly attenuate cable resonances [13]. Since actual power networks show strong resonances, one would underestimate the actual radiation at these frequencies. An alternative would be to design the LISN for a 25- $\Omega$  common-mode impedance. While this smaller impedance would strongly increase the radiation at resonances, there is no certainty that the resonances would occur at the same frequencies in the real installation since the actual power line impedances are unknown. A far-reaching design of an LISN might allow one to adjust the common-mode impedance along the Smith chart to identify the worst-case common-mode impedance for a given DUT. The impact of common-mode impedance on the radiation at resonances should be investigated in future.

Alternatively, it may be worthwhile to further study the PE line impedance in a variety of application areas, for example, in an urban area or in light industry area, and then adjust the LISN impedance according to the application.

## VI. CONCLUSION

An analysis of an imbalanced two- or three-wire VHF LISN was conducted in terms of its mode conversion and termination impedance. It was demonstrated that an imbalanced termination impedance provides a specified degree of conversion from differential to common mode, which can lead to more representative radiated emission test results. To ensure spectral emission

control, an imbalanced LISN is needed. An imbalanced two- or three-wire VHF LISN was prototyped. The impedances in the prototype had less than 10% error in magnitude and 30° in phase compared to the impedances for an ideal imbalanced LISN, as specified by the working group. A 3-D full-wave simulation was performed to investigate the maximum radiation of a two- or three-wire setups using an imbalanced termination. It was demonstrated that the performance of the prototype leads to less than 3.5-dB error as compared to an ideal imbalanced LISN. In EMC applications, this error threshold is acceptable. It is therefore suggested that the impedance of an imbalanced VHF LISN vary by less than  $\pm 30^\circ$  in phase and  $\pm 10\%$ . For the main cable termination, the standard compliance uncertainty has been considered in CISPR 16-4-1 to be 15.5 dB. This uncertainty has been improved to about 9.5 dB for the proposed prototype. The differential- to common-mode conversion for an imbalanced termination was measured with two power line communication device to be as high as 12 dB considering both current and radiated emissions. Using different power nets inside an anechoic chamber, it was demonstrated that the chamber-to-chamber reproducibility will be much better if an imbalanced LISN is used in every chamber.

## REFERENCES

- [1] *Electromagnetic Compatibility of Multimedia Equipment—Immunity Requirements*, CISPR 35:2016, 2016.
- [2] K. Osabe, N. Kuwabara, and S. Okuyama, “Termination impedance for AC mains cable leaving from EUT area in radiated emission measurement,” in *Proc. Int. Symp. Electromagn. Compat.*, Angers, France, 2017, pp. 1–6.
- [3] S. Okuyama, K. Osabe, N. Kuwabara, and H. Muramatsu, “Influence of disturbance current mode on correlation between radiation test sites using VHF-LISN and CMAD,” in *Proc. Int. Symp. Electromagn. Compat.*, Amsterdam, The Netherlands, 2018, pp. 494–499.
- [4] C. Miyazaki, K. Tanakajima, and M. Yamaguchi, “A round-robin test on effectiveness of a VHF LISN for radiated emission measurements,” in *Proc. IEEE Int. Symp. Electromagn. Compat.*, 2011, pp. 14–19.
- [5] S. Okuyama, K. Osabe, K. Tanakajima, and H. Muramatsu, “Investigation on effectiveness of very high frequency line impedance stabilization network (VHF-LISN) for measurement reproducibility,” in *Proc. Int. Symp. Electromagn. Compat.*, 2013, pp. 174–179.
- [6] S. Okuyama, N. Kuwabara, M. Yamaguchi, and K. Osabe, “Improvement in the reproducibility of radiated emission measurements in a fully anechoic room by using VHF-LISN to control the termination condition of the AC mains cable leaving the EUT,” in *Proc. Asia-Pacific Int. Symp. Electromagn. Compat.*, 2016, pp. 50–52.
- [7] S. Okuyama, N. Kuwabara, K. Osabe, and H. Muramatsu, “Improvement of radiated emission measurement reproducibility with VHF-LISN obtained from final results of international inter-laboratory comparison on termination control of power line,” in *Proc. Asia-Pacific Symp. Electromagn. Compat.*, 2015, pp. 589–592.
- [8] C. Miyazaki, K. Tanakajima, M. Yamaguchi, S. Satake, and J. Kawano, “Improvement of dispersion of radiated emission measurement results by VHF-LISN,” in *Proc. IEEE Int. Symp. Electromagn. Compat.*, 2008, pp. 1–4.
- [9] Y. C. Tang, J. S. Chen, C. H. Lee, and C. N. Chiu, “A case study on the consistency improvement in radiated-emission testing by using LISN,” in *Proc. Int. Symp. Electromagn. Compat.*, 2014, pp. 259–262.
- [10] *Artificial Mains Networks for the Boundary of the EMC Test Volume*, CISPR/I/WG2, Aug. 2017.
- [11] D. M. Lauder and R. C. Marshall, “Measurement uncertainty and cable balance—With implications for the CDNE-M and CMAD,” in *Proc. Int. Symp. Electromagn. Compat.*, 2014, pp. 801–806.
- [12] D. M. Lauder and R. C. Marshall, “Measurement uncertainty and cable balance—with implications for the CDNE-M,” in *Proc. Int. Symp. Electromagn. Compat.*, May 2014, pp. 251–254.



- [13] S. B. Worm, "On the relation between radiated and conducted RF emission tests," in *Proc. 13th Int., Zurich Symp. Tech. Exhib. EMC*, 1999, pp. 515–520.
- [14] M. Sørensen, O. Franek, S. K. Christensen, G. F. Pedersen, and H. Ebert, "Assessment of the usability of the workbench faraday cage method," in *Proc. IEEE Int. Symp. Electromagn. Compat.*, 2011, pp. 399–404.
- [15] R. Thompson and D. Knight, "Comparing NPL measurements between OATS and GTEM," *NPL*, Jul. 2008.
- [16] Advance Design System (ADS), 2020. [Online]. Available: <https://www.keysight.com>
- [17] *Specifications for Radio Disturbance and Immunity Measuring Apparatus and Method*, CISPR/TR 16-1-2, 2006.
- [18] CST Microwave Studio, 2020. [Online]. Available: <https://www.cst.com>
- [19] CST Microwave Studio, 2020. [Online]. Available: <https://www.cst.com/company/news/press-releases/agilent-technologies-and-cst-announce-integration-advances-for-rf-and-microwave-circuit-design>
- [20] K. Osabe, N. Kuwabara, and H. Muramatsu, "Impacts to measurement uncertainty of radiated EMI measurement by setting terminating condition of AC mains cable leaving from test area," in *Proc. IEEE Asia-Pacific Symp. Electromagn. Compat.*, May 2018, pp. 52–56.
- [21] *Specifications for Radio Disturbance and Immunity Measuring Apparatus and Method—Part 4-1: Uncertainties, Statistics and Limit Modelling—Uncertainties in Standardized EMC Tests*, CISPR/TR 16-4-1, 2009, .



**Hossein Rezaei** (Member, IEEE) received the B.S. degree in electrical engineering from Islamic Azad University Najafabad Branch, Najafabad, Iran, in 2004, the M.S. degree in electrical engineering from the Shiraz University of Technology, Shiraz, Iran, in 2011, and the Ph.D. degree in electrical engineering from the EMC Laboratory, Missouri University of Science and Technology, Rolla, MO, USA, in 2021.

From 2020 to 2021, he was with ESDMC Technology LLC, Rolla, MO, USA, on developing ESD testing solutions. In April 2021, he joined Intel, Folsom, CA, USA. His research interests include electromagnetic compatibility, signal integrity, electromagnetic susceptibility, RF designs, numerical simulations, and electrostatic discharge.



**Morten Sørensen** (Senior Member, IEEE) received the M.S. degree in physics from Aarhus University, Aarhus, Denmark, in 2005, and the Ph.D. degree in electrical engineering from Aalborg University, Aalborg, Denmark, in 2018.

From 2006 to 2017, he was an EMC and Antenna Specialist with Bang and Olufsen, Struer, Denmark, including three years, from 2011 to 2014, as a Researcher and Technical Project Manager in the innovation consortium, "EMC Design—First Time Right." From 2017 to 2019, he was a Visiting Assistant Research Professor with the EMC Laboratory, Missouri University of Science and Technology, Rolla, MO, USA. Since June 2019, he has been an Associate Professor with the Centre for Industrial Electronics, University of Southern Denmark, Odense, Denmark. His current research interests include near-field scanning, RF designs, electrostatic discharge, and system-level radiated emission.



**Wei Huang** (Member, IEEE) received the B.S. degree from the Beijing University of Posts and Telecommunications, Beijing, China, in 2007, and the M.S. degree from the Missouri University of Science and Technology, Rolla, MO, USA, in 2010, both in electrical engineering.

He was a Research Assistant with the MS&T EMCLAB with interests of electromagnetic, electrostatic, high voltage, and RF designs. He is the Founder of ESDMC Technology LLC, Rolla, MO, USA, and has been focusing on new ESD and EMC test

solutions' developments.



**Daryl G. Beetner** (Senior Member, IEEE) received the B.S. degree in electrical engineering from Southern Illinois University, Edwardsville, IL, USA, in 1990, and the M.S. and D.Sc. degrees in electrical engineering from Washington University, St. Louis, MO, USA, in 1994 and 1997, respectively.

He is currently a Professor of electrical and computer engineering with the Missouri University of Science and Technology, Rolla, MO, USA, is the Former Chair of the Missouri S&T ECE Department, is the Director of the Missouri S&T Electromagnetic

Compatibility Laboratory, and is the Director of the National Science Foundation Industry/University Cooperative Research Center for Electromagnetic Compatibility. He has authored more than 150 research papers, two book chapters, and multiple patents/invention disclosures, receiving several best paper awards or nominations. His research interests include electromagnetic immunity and emissions from the integrated circuit to the system level.

Dr. Beetner was the recipient of the IEEE EMC Society Technical Achievement Award in August of 2020 and was the IEEE-HKN C. Holmes MacDonald Outstanding Young Electrical Engineering Professor in 2003. He has served the IEEE EMC Society as the University Grants Committee Chair, SC-5 Special Committee on Power Electronics Secretary, Educational Committee Secretary and the Vice-Chair, Tutorials Chair, and as the TC-4 Electromagnetic Interference Control Secretary, and served IEEE as an Associate Editor for the IEEE TRANSACTIONS ON INSTRUMENTATION AND MEASUREMENT and as the Chair for the IEEE Medal for Environmental and Safety Technologies Selection Committee. He also served as the Chair of the Central States ECE Department Heads Association.



**David Pommerenke** (Fellow, IEEE) received the Diploma and Ph.D. degree in electrical engineering from the Technical University Berlin, Berlin, Germany, in 1989 and 1995, respectively.

After working with Hewlett Packard for five years, he joined the Electromagnetic Compatibility Laboratory, Missouri University of Science and Technology, Rolla, MO, USA, in 2001 and changed to CTO at ESDMC in 2019. Since 2020, he has been a Professor with the Graz University of Technology, Graz, Austria, in the EMC and RF Coexistence Laboratory.

He has coauthored more than 200 journal papers and is inventor on 13 patents. His research interests include EMC, RF interoperability, system-level ESD, electronics, numerical simulations, EMC measurement methods, and instrumentations.

Dr. Pommerenke is an Associated Editor for the IEEE TRANSACTIONS ON ELECTROMAGNETIC COMPATIBILITY.